

# The Effect of Subcellular Localization on the Oncoapoptotic Capability of Porcine Circovirus Type 1 VP3

A Major Qualifying Project Submitted to the Faculty of

WORCESTER POLYTECHNIC INSTITUTE

in partial fulfillment of the requirements for the

Degree of Bachelor of Science

By

---

Andrew M. Rogers  
Chemistry and Biochemistry

---

Kenneth P. Hough  
Biochemistry

April 26, 2012  
Approved:

---

Dr. Destin Heilman, Primary Advisor (Biochemistry)  
Department of Chemistry and Biochemistry, WPI

---

Dr. Kristin Wobbe, Secondary Advisor (Chemistry)  
Department of Chemistry and Biochemistry, WPI

## **Abstract**

Cancer plagues millions of people in the United States each year. Even with localized irradiation normal cells are still affected by the toxic effects of the therapy. Additionally, pharmaceuticals that target cancer cells are becoming more and more ineffective due to mutations to their target proteins. Interestingly, nature seems to have a solution, through oncotropic, oncolytic, and oncoapoptotic viruses. Apoptin, for example, from the Chicken Anemia Virus (CAV), is known to induce apoptosis in transformed cells by nuclear localization and signaling through the DNA Damage Response pathway. Porcine Circovirus type 1 (PCV1) is another virus from the same family with close homology to CAV. However, the third open reading frame (ORF3) in PCV1, which codes for the third viral protein (VP3), has an extended sequence, making it twice as long as Apoptin. To determine if PCV1 VP3 behaves similarly to Apoptin, several *in silico* and *in vivo* experiments were performed. Localization analysis of PCV1 VP3 reveals cytoplasmic localization in both primary and transformed cells, contrary to Apoptin, which localized in the nucleus. These results suggest an alternative mechanism of apoptosis induction in transformed cells from CAV Apoptin, perhaps directly through the mitochondria, which may be beneficial for future cancer treatment research.

# Table of Contents

<b>ABSTRACT.....</b>	<b>I</b>
<b>TABLE OF CONTENTS.....</b>	<b>II</b>
<b>TABLE OF TABLES.....</b>	<b>III</b>
<b>TABLE OF FIGURES.....</b>	<b>III</b>
<b>ACKNOWLEDGEMENTS.....</b>	<b>IV</b>
<b>INTRODUCTION.....</b>	<b>1</b>
<b>MATERIALS AND METHODS .....</b>	<b>10</b>
<b>RESULTS .....</b>	<b>16</b>
<b>DISCUSSION .....</b>	<b>20</b>
<b>FIGURES AND TABLES .....</b>	<b>24</b>
<b>REFERENCES.....</b>	<b>30</b>

## Table of Tables

TABLE 1: PCR PRIMERS USED IN CLONING. ....	24
TABLE 2: SUBCELLULAR LOCALIZATION PREDICTION (WOLF PSORT) PREDICTS MITOCHONDRIAL LOCALIZATION. ...	25

## Table of Figures

FIGURE 1: AN OPEN READING FRAME PREDICTION ALGORITHM REVEALS A THIRD POTENTIAL OPEN READING FRAME. 24	
FIGURE 2: A PROTEIN SEQUENCE ALIGNMENT REVEALS A 62% PROTEIN HOMOMOLOGY BETWEEN PCV1 VP3 AND PCV2 VP3.....	24
FIGURE 3: A NES PREDICTION ALGORITHM (NESBASE) PREDICTS TWO NESES IN PCV1 VP3. ....	25
FIGURE 4: A RESTRICTION DIGEST VERIFIES THE PLASMIDS ARE OF THE EXPECTED SIZE AND NOT CROSS- CONTAMINATED. ....	25
FIGURE 5: FLUORESCENCE MICROSCOPY OF N-TERMINAL TAGGED GFP FUSION PROTEINS DEMONSTRATES A NON- NUCLEAR LOCALIZATION. ....	26
FIGURE 6: SUBCELLULAR LOCALIZATION OF PCV1 VP3 DOES NOT DIFFER BETWEEN PRIMARY AND TRANSFORMED CELLS. ....	27
FIGURE 7: MITOTRACKER RESULTS INDICATED THERE WAS A POTENTIAL FOR MITOCHONDRIAL LOCALIZATION. ....	28
FIGURE 8: APOPTOSIS INDUCTION IS SELECTIVE TO TRANSFORMED CELLS. ....	29

## **Acknowledgements**

First and foremost, we would like to thank Dr. Destin Heilman for his extreme patience and guidance in both the research and preparation of this manuscript. His guidance was invaluable throughout the project. We would also like to thank Megan Paris and Matija Zelic for providing the foundation behind our research and providing the primary cell localization and apoptosis results. Lastly, we would like to thank Professor Glenn Gaudette (BME), for granting us access to his fluorescent microscope, and Abbie White (BBT), for her constant effort in maintaining the lab.

## Introduction

Cancer plagues millions of people in the United States each year (16). Cancer, also known as malignant neoplasm or carcinoma, is a disease that results from uncontrolled growth of cells, which become highly metabolically active. This can be caused by a variety of reasons, such as: exposure to ionizing radiation (i.e. Ultraviolet radiation, gamma radiation), exposure to toxic chemicals (i.e. tar from cigarette smoke, benzene, vinyl chloride, growth hormones), exposure to certain viruses and bacteria (Human papillomavirus, Hepatitis B and C viruses, Human immunodeficiency virus, Helicobacter pylori), being genetically predisposed to lack certain critical cellular repair and maintenance functions, or malnutrition (5, 34, 34).

Cancer cells require nutrients just like any other cell. However, what makes them unique from normal cells is their extreme need for them. Malignant tumors are often found with new blood vessels running throughout them in order to supply their increased demand for nutrition. This is very characteristic of many cancers tumors, except for leukemia (6). Furthermore, morphologically, cancer cells also have unique features. The nuclei of cancer cells tend to be oblong compared to normal cell nuclei, which are round. This peculiar shape of cancer cell nuclei is due to the high metabolic activity. Cancer cells complete replication at a very fast pace, requiring the up regulation and extensive production of transcription and replication associated proteins. These proteins accumulate in the nuclei of cancer cells giving them their unique shape. In addition to enlarged nuclei, certain cancer cells develop grooves, clefts, indentations or folds on the surface of the nuclei (63). In order for these malignant cells to proliferate constantly, they must circumvent or disable cell cycle checkpoints, such as DNA damage detection and repair, protein ubiquitination and degradation, and replication cycle responses (52). When these suppressors are turned-off, cancer cells often acquire multiple copies of their chromosomes during anaphase. For example, recent findings have shown that failed recognition of damaged DNA, which does not result in DNA repair or apoptosis, can lead to securin-induced

aneuploidy(26). Additionally, benzo[ $\alpha$ ]pyrene, one of the sixty carcinogens found in Tabaco smoke can also induce aneuploidy in mice lacking DNA repair mechanisms (60). These results suggest the importance of cell cycle control. However, merely turning off cell cycle checkpoints is not enough to make a cell malignant. Benign tumors are cells that have proliferated out of control until they have reached senescence, which is the maximum number of cell divisions they can go through. This phenomenon is described by the Hayflick limit, which results from the shortening of the telomeres after each DNA replication. In order for healthy cells to become truly malignant cells, they must replace the shortened telomeres. Cancer cells have been shown to reactivate telomerase making them immortalized (38). Immortalized cells do not follow the Hayflick limit phenomenon, thus they can proliferate limitlessly, however they are neither transformed nor tumorigenic. Further mutations and/or deregulation of proteins or genes result in transformation, where aberrant behaviors of the cell are seen. For example, transformed chick fibroblasts are found to need less insulin-like growth factors for cell multiplication than normal chick fibroblasts (46, 54). Additional mutation in cell cycle control proteins may lead the cell to become tumorigenic, where it proliferates uncontrollably. Once the many mutations required for tumorigenesis occur, the cells can rapidly multiply and spread, similar to the serially multiplying and mutating cells represented in Bert Vogelstein's Vogelgram (20, 46). As the cells progress from microtumors to larger tumors, they become a health issue for the patient and require treatment.

Traditionally, surgical removal of tumors, malignant or benign, was performed. However, tumors that have metastasized or were found in inoperable locations must receive an alternative form of treatment. Non-surgical treatments must induce apoptosis (or programmed cell death) in such cells in order for the post-apoptotic cellular debris to be cleaned up by the immune system. Radiation therapy can be directed to the tumor causing DNA damage and thus apoptosis, but this will still affect surrounding normal cells (3, 7, 59). Current chemotherapies that harness the

power of apoptosis commonly target p53, or similar pathway, in transformed cells (7, 18). p53 plays a role in the intrinsic pathway of apoptosis where DNA damage can trigger it to cause G1 cell cycle arrest and programmed cell death (52). Interestingly, many cancer cells are found to mutate or lack the p53 gene in order to evade the lethal effects of cancer treatment (37, 51). For example, doxorubicin, a commonly prescribed chemotherapy that exploits the p53 pathway to apoptosis, became ineffective against breast cancer cells because of a p53 mutation (1, 35). Fortunately, apoptosis is a complex process that can be induced in a variety of methods.

There are two distinct pathways for apoptosis: extrinsic and intrinsic. In both pathways, apoptosis depends on a cascade of proteolytic cleavages by proteases. The proteases involved in apoptosis have a cysteine residue at their active site that targets specific aspartic acid residues. Because of this the protease was named C(ystein)ASP(artic)ase – caspase (7, 19). Caspase usually exists as a zymogen called procaspase. It is activated by proteolytic cleavage of specific aspartic acid residues by initiator caspases, which are activated by intrinsic removal of the prodomain of initiator caspases. The removal mechanism of the prodomain of initiator caspases depends on the type of apoptotic pathway (9, 19).

The extrinsic pathway is the activation of apoptosis by the extracellular death receptors (19). Cells can enter the apoptotic pathway by death signaling originating from killer lymphocytes, for example, by Fas activation. Upon binding of the Fas ligand with the Fas death receptor, procaspase-8 or 10 are recruited along with Fas-associated death domain (FADD) adaptor protein. The FADD adaptor protein binds the cytosolic domain of the Fas death receptor with procaspase-8 or 10, forming the death-inducing signaling complex (DISC). The close proximity of the procaspases in DISC is sufficient enough to cause cleavage of the adjacent procaspase prodomains, leading to an irreversible activation cascade of caspases (39, 40, 42). AS the extrinsic pathway requires external stimulus, drug designs focusing on this pathway would face a challenge to ensure cancer specificity and reduce cytotoxicity for normal cells.

The intrinsic pathway, however, is the activation of apoptosis from within the cell and thus a much more logical choice for cancer treatment. This pathway can be activated by cellular stress, such as DNA damage, through p53 and PUMA. p53 regulates the Bcl-2 family of proteins and BAX to induce apoptosis (7, 19). The pathway depends on the eventual release of a crucial protein, cytochrome c, from the mitochondria by BAX and BAK for the initiation of procaspases. Cytochrome C binds to a procaspase-activating adaptor called apoptotic protease activating factor-1 (Apaf1). The cytochrome C bound Apaf1 forms a pentameric complex, which recruits procaspase-9 by the caspase recruitment domain. Similar to the activation of caspase in the extrinsic pathway, proximity of the procaspases is sufficient to cause cleavage of the adjacent prodomains (32).

The intrinsic pathway is tightly regulated, thus provides many targets for pharmaceutical intervention. A major family of proteins that participate in the regulation of the intrinsic apoptosis pathway is the Bcl-2 family of regulatory proteins. These contain both pro-apoptotic and anti-apoptotic proteins. Pro-apoptotic proteins enhance cytochrome C release by forming a heteromeric pore in the mitochondrial membrane (7, 11, 19, 62). They are also capable of creating such pores in the ER causing an influx of  $Ca^{2+}$  ions, enhancing the apoptotic pathway through calpain and the activation of tissue transglutaminase (43).

These various pathways of apoptosis induction can be studied to develop a synthetic drug that can kill transformed cells. A ground up design of a de novo chemical targeting cancer cells can be an overwhelming task. However, the synthesis of a drug that mimics the functionalities of an already existing protein in nature may be a more ideal solution. For example, Viruses have evolved a specific tropism, or ability to select for cells that would promote viral propagation. It is possible that nature has evolved viruses that are specific to transformed cells. In fact several viruses have already been characterized to have oncotropic properties. The autonomous parvovirus, for instance, is not only oncotropic (targeting cancer cells for infection)

but also is oncolytic (lyses the cell for proliferation) (13). In particular, a group of researcher in 1999 engineered a herpes simplex virus type-1 (HSV-1), which is known to be oncotropic, oncolytic and contain an intact *HSV-TK* gene, with an exogenous *CYP2B1* gene that encodes for the cyclophosphamide sensitive rat cytochrome P450 2B1 enzyme. Thus the new engineered virus can catalyzes the cyclophosphamide chemotherapy to its active form with the rat cytochrome P450 2B1. In addition to drug activation, ganciclovir prevents the cell from repairing the DNA damage cyclophosphamide causes, eventually killing the cell if the lysis did not occur from the virus itself (3).

While this approach provides an interesting idea, it is still subject to the forces of evolution and could result in the loss of ocotropism. Should this occur, the virus could infect and kill healthy cells creating a huge risk for clinical use. For this reason, it may be better to investigate individual proteins that could confer this activity, rather than whole viruses. However there are potential pit falls to this idea as well. For example, if the mechanism of cancer cell detection and death induction resides in the nucleus, it is very hard to engineer a molecule that has the required functionalities while still being small enough to enter the nucleus. With that said, the pursuit of such proteins should not be hindered since there may be alternative pathways to the end result.

One such protein, that has onco-specific activity, has been isolated from Chicken Anemia Virus (CAV). CAV produces a third viral protein (VP3) called Apoptin(41). The presence of the well-characterized VP3 in CAV, has raised the question on if the rest of the family – circoviridae- also has this third viral protein. This family of viruses is classified by a small, circular, single stranded, ambisense DNA(45). The viroids are non-enveloped, spherical in structure and are known to autonomously replicate in infected eukaryotic cells(14). The family is broken down to two different genera: *circovirus* and *gyrovirus*. The genus *circovirus* is currently comprised of Beak and Feather Disease Virus (BDFV), Canary Circovirus (CaCV),

Duck Circovirus, Finch Circovirus, Goose Circovirus (GoCV), Gull Circovirus, Pigeon Circovirus (PiCV), Porcine Circovirus 1 (PCV1), Porcine Circovirus 2a (PCV2a), Porcine Circovirus 2b (PCV2b), Starling Circovirus and Swan Circovirus. While the *circovirus* genus has eleven members, the *gyrovirus* genus solely contains CAV(64). With such a large family of viruses, the question arises why is CAV so well characterized.

CAV was found to be the etiologic agent of a disease in young chickens that resulted in anemia, lymphoid depletion and hemorrhaging and thus can affect food sources(14). Genomic analysis has shown It contains a closed circular, single stranded DNA of approximately 2300 nucleotides with three open reading frames (ORF)(14, 22, 45). Each of the three ORFs code for a viral protein designated VP1, VP2 and VP3. VP1 is a 51kDa capsid protein and VP2 is a 24KDa phosphatase(36). VP3 is a 13.5kDa protein, and was renamed Apoptin because of its apoptotic activity in cells. This activity has been attributed to be the cause of anemia in chickens due to triggering apoptosis in infected thymocytes and eruthroblasts. Furthermore, Apoptin was found to induce apoptosis in transformed human cells in a p53 independent manner(41, 55).

Apoptosis induction has be found to be caused by apotpin interacting with the APC1 subunit of the Anaphase Promoting Complex/Cyclosome (APC/C)(22). Furthermore, Apoptin must localize to the nucleus to confer this effect. Examination of the protin for signaling sequences has identified an active bipartite Nuclear Localization Sequence (NLS), found near the C-terminus of the protein(15). In addition, the activity of this NLS has been shown to be mediated by the IMP $\beta$ 1 protein of importins (IMP). IMP $\beta$ 1 binds to the NLS of Apoptin in the cytoplasm and translocates through the Nuclear Pore Complex (NPC) in to the nucleus. It is then released by the binding of RanGTP to IMP $\beta$ 1(4).

A NLS usually consists of one or two short sequences that are either lysine or arginine rich, and can be found on the surface of the folded protein. This facilitates the selection of proteins that enter the nucleus, which are too large to enter through the Nuclear Pore

Complex(2). The reverse process, observed with apoptin in primary cells, is mediated by a nuclear export sequence (NES), found on proteins that need to be exported from the nucleus(21).

In Apoptin, the bipartite NLS was proven to be functional in an experiment where point mutations were made at different location of the bipartite NLS. The results showed that the mutant NLS caused Apoptin to be mislocated to the cytoplasm instead of the nucleus(22). In addition to the NLS, Apoptin has a NES between amino acids 33 and 46. This NES was also shown to be functional by the same means of point mutation, and mislocation of the mutant protein. The sequence was also found to be CRM1-dependent, one of the exportin proteins.

Apoptin's ability to induce apoptosis selectively in transformed cells has been shown to be mediated by its distinct nuclear localization for transformed cells, and cytoplasmic localization for primary and non-transformed cells (22, 41). Recent studies suggest that the localization of Apoptin to the nucleus is mediated by its capability to interact with the cell's DNA Damage Response pathway (28). It is not surprising to find viruses that encode proteins capable of manipulating the cell cycle. A virus may block a cell from apoptosis, induce S phase in order to replicate its genome, or may induce G2/M arrest supporting viral egress (23).

If CAV expresses a protein that manipulates the cell cycle, it is not improper to presume that other members of the *Circoviridae* family do as well. The Porcine Circovirus (PCV) is the representative virus of the genus circovirus, the other genus in the *Circoviridae* family (47). Originally discovered in 1974 by Tischer, et. al. from a porcine kidney cell line PK/15 (ATCC CCL 33) (57, 58), PCV was classified as non-pathogenic until the discovery of another PCV-like virus in North America that was determined to be the etiologic agent of Postweaning Multisystemic Wasting Syndrome (PMWS) in swine (17, 56). The symptoms of PMWS include anemia, diarrhea, dyspnea or tachypnea, hepatitis, interstitial pneumonia, lymphadenopathy, nephritis, and progressive weight loss in young pigs making it similar to the pathology observed

in CAV. The new strains were found to be genomically diverse when compared to the original PCV isolate (now known as PCV1) and was named PCV type 2 (PCV2). PCV2 is further divided into two serotypes, 2a and 2b with different associated pathophysiology. PCV1 and PCV2 all have a closed, circular, single-stranded DNA genome, with a size of 1759 nucleotides for PCV1 and 1767 nucleotides for PCV2. Both viruses express two open reading frames that have been shown to be relatively homologous. Recently a third ORF has been located in both viruses that is significantly different between PCV1 and both PCV2 serotypes. For PCV2, ORF3 is 315 nucleotides, while PCV1 is 621 nucleotides, resulting in an extended tail when compared to PCV2 (17).

A whole genome sequence alignment performed with CLUSTALW2 Multiple Sequence Alignment 2.1 resulted in a sequence homology of 95% between PCV2a and PCV2b, 78% between PCV1 and both PCV2, 55% between PCV1 and CAV, 55% between PCV2a and CAV, and 53% between PCV2b and CAV(31). Furthermore, among the PCVs, the primary difference in the Viral Protein 3 (VP3) sequence is an extended C-terminus for PCV1 VP3, giving it a “tail”. There is a 61.5% homology in VP3 sequences between the two PCV2 and PCV1 (33). Furthermore, PCV2a and PCV2b both have putative NES and NLS sequences as was previously shown. Further, it was shown that the NES and NLS signals were functional in PCV2a, but only the NES was definitively shown to be functional in PCV2b (53).

The high degree of homology suggests VP3 may have a similar function to apoptin. Recently, VP3 of PCV2 has been identified to induce apoptosis as well. Its mechanism of induction is through the caspase 8 and caspase 3 pathway and has been shown to be p53 mediated(33). This is contrary to its homolog protein, Apoptin, which is known to induce apoptosis in a p53-independent manner (22). However, in a another recent study, PCV2 VP3 was shown to induce apoptosis in a p53 null transformed cell line, proving that it is p53 independent (27).

With the aforementioned in consideration, this study investigates whether a relatively uncharacterized virus, Porcine Circovirus 1, from the same family codes a homologous protein with similar function. As stated earlier, sequence analysis results revealed a putative third open reading frame (ORF3) that shared decent homology with CAV's ORF3, except with an extended "tail" sequence doubling its length. Subcellular localization of wild type and truncated VP3 and apoptosis assays of wild type VP3 were performed to unveil the protein's function in comparison to Apoptin.

## **Materials and Methods**

### **Bioinformatics and Sequence Analysis**

An open reading frame prediction algorithm was used to find open reading frames within the PCV1 genome consisting of at least 100 codons (MacVector). The nucleotide sequence of the third predicted reading frame was translated to protein sequence and aligned with the third ORF of PCV2a and PCV2b. PCV1 ORF3 was also searched for known signal motifs and predicted subcellular localization patterns (WoLFPSORT)(24). Additionally, an NES prediction program was used to determine the probability of an NES within PCV1 VP3 and PCV2a/b VP3 (NESBase)(29).

### **PCR Amplification and Purification**

PCR amplification of PCV1 ORF3 segments was performed using the GoTaq® Green Master Mix (Promega, Madison WI) under the following conditions: dsDNA melting (95°C, 30s), primer annealing (55°C, 30s), and extension (72°C, 30s). Following 30 cycles the reaction was held at 72°C for a final extension for 1 min then cooled to 10°C for storage. Forward and reverse primers were previously engineered to amplify the full-length third open reading frame as well as four truncation mutants representing the putative NLS, Tail, Forward section, and a segment consisting of the NLS and Tail sections (Table 1)(44). Each engineered primer included an EcoRI restriction site in the forward primer and a BamHI restriction site in the reverse primer. Following PCR amplification each reaction was loaded on a 0.9% agarose gel in 1xTAE buffer. Bands consistent with the size of each fragment, as compared to a size marker (New England Biolabs 2-Log Ladder, Cat N3200L) were excised.

### **Plasmid Ligations**

PCR products were ligated into pGEM® T-Vector for stabilization prior to ligation into the appropriate expression vector. pGEM ligations were performed using the Promega Easy T-Vector Kit. Reactions were prepared using a insert:vector ration of 3:1 followed by incubation at

4°C for 24-48 hours. Expression vector ligations into pEGFP-C1 and p3xFLAG-myc-CMV-26 (Clontech, Palo Alto CA) were performed at a 4:1 insert:vector ratio with 3u T4 DNA Ligase (Promega, Madison WI) in buffer supplied by the manufacturer at EcoRI and BamHI restriction sites.

### **Transformation of Competent *E. coli***

Overnight ligation products (5µL) were added to JM109 competent cells (50µL, >108cfu/µg, Promega cat. L2001). The cells were then incubated on ice for 15 minutes and followed with a 60 second heat shock at 42°C. The samples were placed on ice for 2-minutes. LB broth (450µL) was added and the cells incubated at 37°C for 1 hour. Plates for overnight growth were prepared by spreading IPTG (100mM, 40uL) and x-gal (50mM, 20uL) on LB Agar plates with 50µg/mL of appropriate antibiotic (IPTG and x-gal only used for pGEM ligation products). These plates were incubated at 37°C until no longer runny. Following 1 hour at 37°C, the transformed *E. coli* was plated and incubated at 37°C overnight (12-18 hours).

### **Quick Colony Screening**

Colonies (8-10 per plate, white colonies only in the case of pGEM) were picked and 20µL ddH<sub>2</sub>O inoculated and a replica plate prepared. A passive-lysis buffer (56mM NaOH, 1% SDS, and 6mM EDTA in ddH<sub>2</sub>O) was prepared and added (20µL) to each inoculated sample of ddH<sub>2</sub>O. The resulting solutions were vortexed and then centrifuged at high speed for 30 seconds. The cleared lysate was loaded on a 0.9% agarose gel and run for 2 hours at 90V. Samples suggesting the presence of an insert (elevated from parent plasmid lane) were further analyzed by small-scale purification and restriction.

### **Screening by Small Scale Plasmid Purification**

Definitive colony screening was performed by mini preparation and restriction of purified DNA. Mini preparations were performed from 3mL LB starter cultures (with plasmid-appropriate antibiotic) incubated at 37°C for 8-12 Hours. Each culture was centrifuged at 12,000 x g for 30

sec and the supernatant discarded. The pellet was re-suspended in cold (4°C) MPSI (100µL, 50mM glucose, 25mM TRIS-HCL [pH 8.0], 10mM EDTA). Freshly prepared MPSII (200µL, 0.2M NaOH, 1% SDS) was added, the mixture inverted several times to mix, and incubated on ice for 2 min. MPSIII (150µL, 5M Acetate buffer from KOAc and HOAc [pH 5.2]) was added and the samples gently vortexed. The samples were then incubated on ice for 5 minutes and centrifuged at 12,000 x g for 5 minutes. The supernatant was transferred and the pellet discarded. Ethanol (95%, 900µL) was added and the supernatants and incubated at RT for 5 minutes. The samples were centrifuged at 12,000 x g for 5 minutes, the supernatants discarded and the pellets air-dried. The pellets were washed with ethanol (1ml, 70%), centrifuged and air dried as previously described, and re-suspended in sterile 1xTE (50µL). Purified DNA was subjected to restriction digests as described below.

#### **Medium Scale Plasmid Purification (Midi Preparation)**

Overnight cultures were inoculated with 200µL of 3mL starter cultures with restriction profiles consistent with the desired insert. The overnight cultures were then incubated 16-18 hours at 37°C to an OD<sub>600</sub> of 1.5-2.2. Plasmid DNA was isolated using a PureYield™ Plasmid Midiprep System (Promega) via the published protocol(49) using the elution by centrifugation protocol and an elution volume of 600µL sterile 1xTE.

#### **Restriction Digests**

All restriction digestions were performed in 20µL with 10u BamHI, 10u EcoRI, 1-2µg DNA, 2µL 10x Buffer H (Promega), and 0.5U (500U/mL) RNase A, and 20U (20,000U/mL) RNase T1 (Life Technologies, Grand Island NY). Digestion reactions were incubated for 1-2 hours at 37°C immediately followed by agarose gel electrophoresis on a 0.9-1.0% gel (1-2 hours at 90V).

## **DNA Quantification and Sequencing**

DNA requiring approximate quantification was diluted 100 fold in nuclease free H<sub>2</sub>O and absorbance was measured at 260nm. Approximate concentrations were calculated using an extinction coefficient of 20 L/g•cm. DNA samples for sequencing were prepared by dilution to 100ng/μL and sent for sequencing by Macrogen USA.

## **Cell Culture Maintenance**

H1299 cells of human lung origin (ATCC CRL 5803) lack endogenous p53 expression were maintained in Dulbecco's Modified Eagle Medium (DMEM)/high glucose supplemented with 10% fetal bovine serum (FBS), and PSF (100 units/mL Pen G sodium; 100mg/mL streptomycin sulfate; 0.25 mg/mL amphotericin B) incubated at 37°C and humidified 5% CO<sub>2</sub>. Confluence was maintained at or below 95% by frequent passage. Cultures were discarded after passage 15 and a new stock thawed to minimize the possibility of new mutations from handling.

## **Transient Transfection**

H1299 cells for sub cellular localization studies were transiently transfected with N-terminal tagged EGFP truncation mutants placed under the control of a constitutive CMV promoter using the Qiagen Effectene® Transfection Reagent Kit via the published protocol(50).

## **Fluorescence Microscopy**

H1299 non-small cell lung carcinoma cells were seeded in 6-well plates containing circular coverslips at a confluence (24 hours post seeding) of 30-60%. At a confluence of 75-80% the cells were then transfected as described previously. The following day (24 hours post transfection) the growth media aspirated, the cells washed in 1xPBS, and were fixed with 4% paraformaldehyde under gentle agitation for 15 minutes. In the case of mitochondria staining with MitoTracker Deep Red™ (Invitrogen), MitoTracker was suspended in DMSO and diluted in PBS as described(25), added to each well, and incubated for 30 minutes under gentle agitation

prior to fixation. The cells were then washed in 1xPBS and mounted with 15 $\mu$ L mounting media (50% glycerol; 100mM Tris (pH 7.5); 2% DABCO, 10 $\mu$ g/mL DAPI). The slides were then stored at 4°C for 72 hours and imaged by epifluorescence (nuclear/cytoplasmic) or confocal (mitotracker) microscopy.

### **Nuclear/Cytoplasmic Fraction Determination**

The nuclear/cytoplasmic fraction was calculated for each GFP-tagged construct through analysis of the green histogram with ImageJ (National Institutes of Health, Bethesda, Maryland). The mean green intensity for the nucleus was compared to the mean green intensity of the cytoplasm.

### **Mitochondrial Localization Algorithms (8, 12)**

Mitochondrial localization was calculated using two different algorithms: Van Steensel's Cross Correlation Function (CCF), and Li's Intensity Correlation Analysis (ICA). Van Steensel's CCF calculates for the Pearson's Coefficient of the two channels for each shift in one channel. That is, one channel remains stationary, while the other is shifted in either direction. For our calculations, the GFP channel was shifted over the stationary Mito Tracker® channel and the Pearson's Coefficient was calculated for each shift. The CCF  $\delta x$  for the calculations performed were set to 20 pixels, meaning the GFP channel was shifted up to 20 pixels to the left and right from the center of the image.

The Li's ICA calculates the intensity distribution of the pixels for each channel against the covariance between the channels. The covariance between the channels is calculated as the product of the variances in each channel. The variance in Channel A, for example, is represented as follows,  $\sum_i A_i - a$ , where  $A_i$  is the intensity at a specific pixel  $i$ , and  $a$  is the mean intensity of the channel. The same is performed for the other channel. Thus, if there is an intensity peak in once channel but not in the other, the product will equal zero, meaning no co-

localization. Furthermore, if both channels have peak intensities at the same pixels, the product of the two variances will equal a positive number, and thus a potential for co-localization.

### **Apoptosis Assays**

Cells were seeded at approximately 80% confluence and incubated as described previously. Cells at 80% confluence were transfected as previously described(44) (and above) with p3xFLAG-myc-VP3 constructs to be tested. Twenty-four hours post transfection Caspase-3/7 reagent and buffer (Promega) were added as described(48). At 24 and 48-hours post reagent addition the plate fluorescence was read ( $\lambda_{ex}=499$ ,  $\lambda_{em}=521$ ). Fluorescence intensities were normalized to the vehicle well (as 0).

## Results

### Bioinformatics

**A third open reading frame exists within the PCV1 genome that is highly conserved with the third open reading frame of PCV2.** PCV1 has been characterized to possess two open reading frames. Recently, however, other members of the Circoviridae family have been shown to have a third open reading frame. To investigate whether or not PCV1 contains a third open reading frame, similar to CAV and PCV2, an open reading frame prediction algorithm was run on a representative sample of the PCV 1 total genome (Figure 1). This analysis revealed a third open reading frame consisting of 208 codons and is presumed to express PCV1 VP3. To explore the level of similarity between this third viral protein and that of its sister viral proteins a protein sequence alignment was performed revealing a 62% protein homology between PCV1 VP3 and PCV2 VP3. There are several long homologous domains consisting of extended stretches of conserved amino acids. Additionally, an elongated “tail” domain, almost doubling the length of the protein, was identified (Figure 2). A nucleotide alignment revealed a single nucleotide mutation at nt 315 resulting in a stop codon in PCV2 but a tyrosine in PCV1 (Data not shown). The high degree of homology amongst aa 1-105 (n.t. 1-315) suggests that PCV1 VP3 may be intended to perform the same function as PCV2 VP3.

**PCV1 ORF3 contains several putative signal sequences.** Apoptin, the best-characterized VP3 of the family, has been shown to possess several functioning signal sequences. These signaling sequences have been linked to the selective apoptotic ability in transformed cells. Specifically, apoptin has been shown to require nuclear localization to induce apoptosis and as such is found in the nucleus of transformed cells and cytoplasmic in primary cells. A broad signal sequence prediction algorithm was performed on the protein sequence to determine the (predicted) subcellular localization. The algorithm did not identify any known signal peptides or suggest the presence of new signal peptides and in most cases suggested

cytoplasmic localization (data not shown). A NES prediction program identified a possible NES at aa 42-49 and a strong probability of a NES at 134-149 (Figure 3). Comparison of the sequence in these regions to the published NES consensus sequence (L-(2,3)-[LIVFM]-(2,3)-L-x-[LI])(30) revealed sequences that corresponded to the consensus. The putative NES located in the tail consisted of several iterations of the consensus (data not shown) suggesting a functional NES in the tail confirming cytoplasmic localization.

### **Subcellular localization studies**

**PCV1 VP3 localizes to the cytoplasm in transformed cells.** As Apoptin has been shown to localize to the nucleus in transformed cells and this localization pattern has been linked to its ability to induce apoptosis. Being so closely related, we hypothesized PCV1 VP3 may behave in a similar manner. To investigate this, a series of plasmid constructs containing N-terminal EGFP-tagged fusion proteins were created. Prior to transfection, a double restriction digest was performed to verify plasmid integrity and transfectability (Figure 4). Wild-type ORF3 was transfected into H1299 cells that were fixed and mounted 24 hours post transfection. Epifluorescence imaging of the mounted cells revealed a strong cytoplasmic preference for PCV1 VP3 compared to that of apoptin (Figure 5A). To explore what predicted sequences are responsible for this localization a series of truncation mutants representing each of the putative signal sequences was prepared. These mutants were transfected into H1299s as described previously. Imaging confirmed the suspicion that the tail is directing strict cytoplasmic localization (Figure 5B). Quantification of the epifluorescence images compared to an EGFP control confirmed the visual interpretation (Figure 5C). This striking difference in localization from apoptin suggests PCV1 VP3 selects for and induces apoptosis in a different manner.

**The cytoplasmic localization of PCV1 VP3 is independent of transformed cell status.** The difference in subcellular localization between primary and transformed cells is a well-characterized method of activity selection. Apoptin localization has been shown to differ

between transformed and primary cell lines. This nuclear-cytoplasmic shuttling has been linked to the ability of apoptin to selectively induce apoptosis. To determine if PCV1 VP3 behaves in a smaller, albeit opposite, manner, requiring cytoplasmic localization to induce apoptosis, we compared the localization of EGFP tagged wild-type PCV1 VP3 in primary foreskin fibroblasts (electroporation by Paris, et. Al.)(44) to the previously transfected H1299s. Confocal imaging of the transfectants revealed no difference in subcellular localization between cell types (Figure 6A). Quantification was performed as described previously and confirmed the visual interpretation (Figure 6B). This result suggests that PCV1 VP3 has evolved a separate mechanism of apoptosis selectivity.

**PCV1 VP3 does not localize to the mitochondria in transformed cells.** Several localization prediction algorithms have suggested mitochondrial localization (Table 2). Known to play a large role in the apoptosis pathway, the mitochondria would be a logical target for the induction of apoptosis. To investigate the possibility of mitochondrial localization, H1299 cells were transfected as described previously with wt PCV1 VP3 GFP DNA. Prior to fixation the cells were incubated in Mitotracker™ for 30 min then fixed as previously described. The cells were then visualized by confocal microscopy. Mitotracker™ and EGFP channel merges revealed partial co-localization, however, many regions did not overlap between channels (Figure 7A). To provide a more mathematical analysis of co-localization a Van Steensel's Cross Correlation Function (CCF) analysis was performed. The results indicated a low possibility of co-localization is but unconfirmed (Figure 7B). Further analysis by Li's intensity correlation analysis was used in an attempt to provide a better estimate of co-localization. Again, the results only indicated a potential for co-localization with a significant amount of green bleed through due to a greater green intensity (Figure 7B). Furthermore, noise and difference in channel intensity caused skewing of the results, thus not providing conclusive data. These results suggest that PCV1

VP3, while not localizing to the mitochondria, might interact with the mitochondria, providing a possible starting point to the mechanism of apoptosis selection and induction.

### **Apoptosis Assays**

**PCV1 VP3 selectively induces apoptosis in transformed cell lines.** As the subcellular localization does not differ between primary and transformed cells, the next logical question is does PCV1 VP3 possess the ability to induce apoptosis and is it also selective to transformed cells. To investigate this behavior, PFF cells (by Paris et. Al.) (44) and H1299s were transfected with the p3xFLAG-myc-CMV-26-PCV1-VP3 construct. The Apo-ONE Caspase 3/7 assay was added as previously described and the fluorescence intensity measured. The results indicate that not only does PCV1 VP3 induce apoptosis it does it in a selective manner. PFF induction was normalized to 1, although the difference from background was not statistically significant, H1299 apoptosis induction was 33-fold higher than in PFFs (Figure 8). These results combined with the localization information suggests that not only does PCV1 VP3 also possesses the ability to induce apoptosis selectively in transformed cells, it does so through a different mechanism than apoptin.

## Discussion

Viral proteins like Chicken Anemia Virus (CAV) Apoptin, which induce apoptosis only in transformed cells (41), are important in cancer research. By elucidating the specific mechanism of action of anti-cancer proteins, it is possible to design and develop pharmaceuticals that mimic its function. Such drugs will be only specific to cancer cells, and will hopefully become the standard of cancer treatment, replacing broader ineffective treatments, such as chemotherapy and radiation (37, 61).

CAV has been well characterized for its functionality, localization pattern, and pathways of action(28). However, Porcine Circovirus 1 (PCV1), which is part of the same family as CAV (Circoviridae) (45) is not well known. Sequence analysis of PCV1 and CAV reveals a close homology between them. If the third viral protein (VP3) of PCV1 functions similarly to CAV Apoptin, yet another cancer killing viral protein may shed light to the development of novel cancer specific pharmaceuticals.

The first striking difference noted is the evolution of the tail domain. This domain is unique to PCV1 VP3 when compared to PCV2 and CAV VP3s. In terms of evolutionary need, what does this tail domain offer that would drive it's evolution, or removal? Analysis of PCV1 VP3 through GFP fusion proteins shows strong cytoplasmic localization of PCV1 VP3 where a more diffuse, but still predominantly cytoplasmic, localization for PCV2 VP3. Truncation mutants, representing putative signaling sequences, show the large driving force behind cytoplasmic localization resides within this tail domain. This observation is consistent with the prediction of a NES within this domain. These observations suggest evolution of PCV required the removal or addition of this signal.

The next logical step is to determine if this mutation, is for the gain of a NES, or the removal an NES. Mutants expressing only the forward portion of PCV1 VP3 still remained predominantly cytoplasmic, however, did have some nuclear localization suggesting that a

second signal sequence is present. Comparison of this signal sequence with that observed in PCV2 VP3 shows PCV2 has additional mutations within the predicated NES location. This suggests that PCV2 may have evolved a second NES after the tail was truncated.

Evaluation of the PCV pathogenicity also provides insight to the origin of this tail domain. Many recent studies have suggested that VP3 is linked to the pathogenicity of PCV (10, 33) and, in PCV2, is responsible for the depletion of immune B-cells. In contrast, PCV1 infections tend to be self-limiting and resolve with immune clearance of the virus. This difference in pathophysiology serves to suggest that the tail domain is provides a protective effect and prevents apoptosis induction by PCV1. This gain of function between PCV1 VP3 and PCV2 VP3 suggests that evolution removed this protective tail to enhance viral survival.

Interestingly, some experiments have demonstrated an increase in apoptosis induction amongst PCV1 VP3 transfected cells over PCV2 VP3 transfected cells. These experiments have a distinct disadvantage as they have only been reported in transformed cell lines. In this study we report that PCV1 VP3 has the ability to selectively induce apoptosis in transformed lines. As such, we demonstrate that PCV1 VP3 does not induce apoptosis in primary, or healthy cells. To confirm if the tail domain is inhibiting PCV VP3 apoptotic capability truncation mutant apoptosis experiments should be preformed in primary cells, perhaps PCV2 VP3 is not transformed cell specific in porcine cells.

Comparison of the subcellular localization of PCV1 VP3 to the well-characterized oncoapoptotic protein apoptin could provide insight into the mechanism PCV1 VP3 utilizes to select for and induce apoptosis. The requirement of nuclear-cytoplasmic shuttling to induce apoptosis observed in apotptin is evidently not required in PCV1 VP3. Despite these differences in localization, the apoptosis assay indicated that PCV1 VP3 only induces apoptosis in transformed cells, like Apoptin. This suggests that PCV1 VP3 may be sensing and inducing apoptosis in transformed cells differently than Apoptin.

Apoptin localizes to the nucleus of transformed cells by sensing DNA Damage from the cell's DNA Damage Response (DDR) Signaling. Once in the nucleus it interacts with the Anaphase-Promoting Complex/Cyclosome to induce G2/M cell cycle arrest and apoptosis (55). Although, in the case of PCV1 VP3, the mechanism of specificity for transformed cells is not known, the pathway of apoptosis can be predicted from the assay used for apoptosis detection. First and foremost, the cell line used (H1299) is known to be p53 null, thus it cannot participate in the pathways of induction tied to p53. Secondly, the assay uses cellular Caspase-3/-7 activity to convert a non-fluorescent substrate to a fluorescent one. Thus a potential path of apoptosis may be through the Bcl-2 family of receptors, BAX, or BAK, and the activation of the mitochondrial apoptotic pathway. This results in the release of cytochrome C from the mitochondria, which binds to Apaf-1, activating Caspase-9, then Caspase-3, eventually resulting in DNA fragmentation and cell death (19, 43).

During the cellular localization experiments an unexpected trend was noticed. In the PCV1 VP3 constructs including the tail domain, the GFP-fusion proteins formed a highly vesicular pattern not noticed in the forward domain. Analysis of the tail domain for hydrophobic residues revealed the tail is highly hydrophobic. This suggested that the vesicular pattern might be from multimerization minimizing free energy or interaction with membrane structures, such as the organelles, in the cytoplasm.

The vesicular pattern and the above mentioned apoptotic pathway for PCV1 VP3 raised the question of if the pattern observed was due to co-localization with the mitochondria. Although, PCV1 VP3 mitochondrial co-localization results were inconclusive, the nuclear-cytoplasmic localization and microscopy results strongly suggest an intrinsic mitochondrial dependent pathway of apoptosis from the cytoplasm or the mitochondria (19). This is corroborated by presumed apoptosis pathway of PCV2 VP3 which has been shown to only be cytotoxic to infected/transformed cells (10). Furthermore, the seemingly overlapping channels

between GFP and Mito Tracker® may merely indicate protein interactions between PCV1 VP3 and Bcl-2 family receptors, or even BAX and BAK, which are both directly involved in the permeabilization of the outer mitochondrial membrane (11, 19, 43). Finally, through these results, the role of PCV1 VP3 in intrinsic apoptotic induction has become clearer, but its specific mechanism of sensing transformed cells still needs investigation.

Noteworthy future investigation should revolve around the specific mechanism PCV1 VP3 is using to induce apoptosis and what is conferring transformed cell specificity. More in depth study of PCV1 and PCV2 VP3 activity in primary cells should be conducted to further elucidate what role the tail domain is playing. Co-Imunoprecipitation experiments for tail-associated protein binding and VP3 structure determination may provide a better understanding of this protein's function. Additionally, a comparison of PCV pathogenicity in infected primary and transformed cells independent of the determination of VP3 expression will provide a more in-depth knowledge of protein interactions. Once the particular mechanism PCV1 VP3 uses to select transformed cells and induce apoptosis can be elucidated we will be one step closer to the development of an effective cancer specific drug.

## Figures and Tables

Name	Oligonucleotide sequence (5'-3')	Restriction Site
PCV1-VP3-1F ( <i>VP3-F1</i> )	GCGAATTCAATGATATCCATCCCACC	EcoRI
PCV1-VP3-190F ( <i>NLS-F</i> )	GCGAATTCACACATACGTTACAGGGA	EcoRI
PCV1-VP3-315F ( <i>TAIL-F</i> )	GCGAATTCATATGTGGCCTTCTTTACT	EcoRI
PCV1-VP3-189R ( <i>NES-R</i> )	GCGGATCCTTAAGAAATTTCCGCGGG	BamHI
PCV1-VP3-315R ( <i>NLS-R</i> )	GCGGATCCCTACTTATCGAGTGTGGA	BamHI
PCV1-VP3-622R ( <i>VP3-R</i> )	GCGGATCCTCAGTGAAAATGCCAAG	BamHI

Table 1: PCR primers used in cloning.

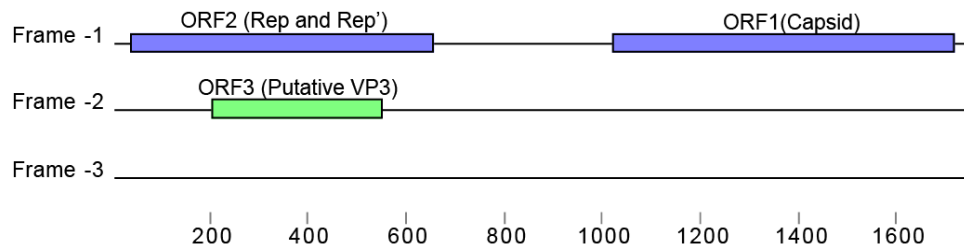


Figure 1: An open reading frame prediction algorithm reveals a third potential open reading frame.

A third ORF, putatively expressing VP3, was identified with MacVector. The search was performed using a minimum count of 100 codons.

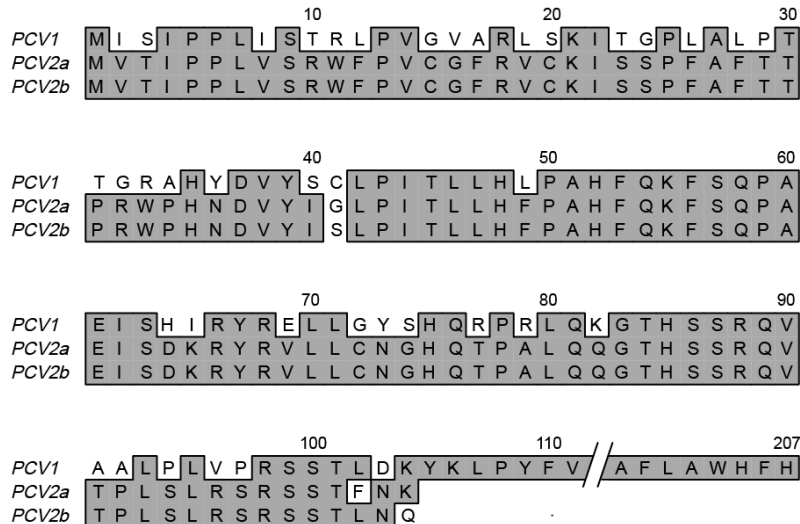


Figure 2: A protein sequence alignment reveals a 62% protein homology between PCV1 VP3 and PCV2 VP3.

In addition to the high-level homology an elongated "tail" domain was found doubling the length of PCV1 VP3 over that of PCV2 VP3.

Subcellular Localization	Probability
Mitochondria	14.0
Peroxisome	7.0
Nucleus	5.0
Cytoplasm	3.0

**Table 2: Subcellular localization prediction (Wolf PSORT) predicts mitochondrial localization.**

(K-NN=32, Threshold=25)

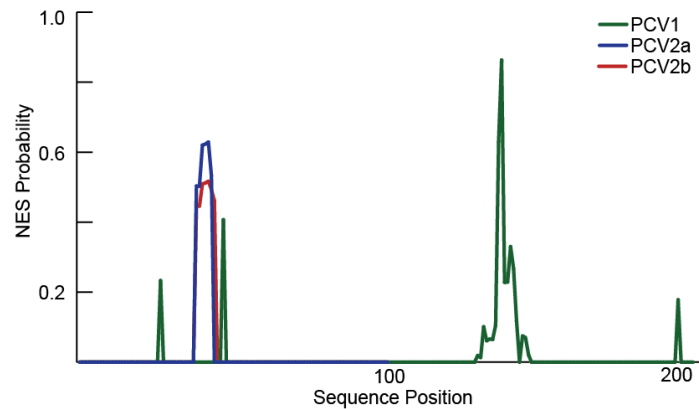


**Figure 3: A NES prediction algorithm (NESBase) predicts two NESes in PCV1 VP3.**

For each PCV type a NES was weakly predicted in the forward region. In the case of PCV1 VP3, a strong NES was predicted in the tail domain. (Probability threshold = 0.5)

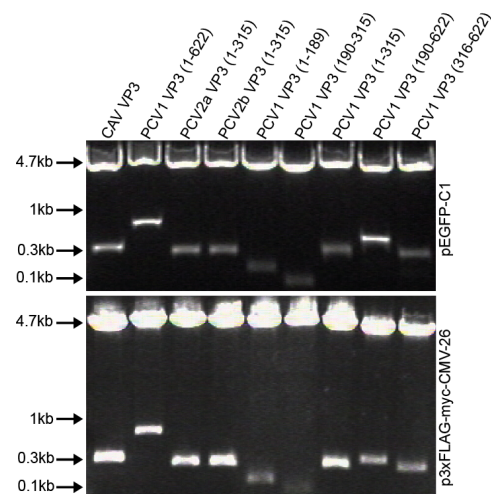


**Figure 4: A restriction digest verifies the plasmids are of the expected size and not cross-contaminated.**

An EcoRI and BamHI restriction digest purified by agarose gel electrophoresis verifies the plasmids were free of cross contamination and of the expected size.

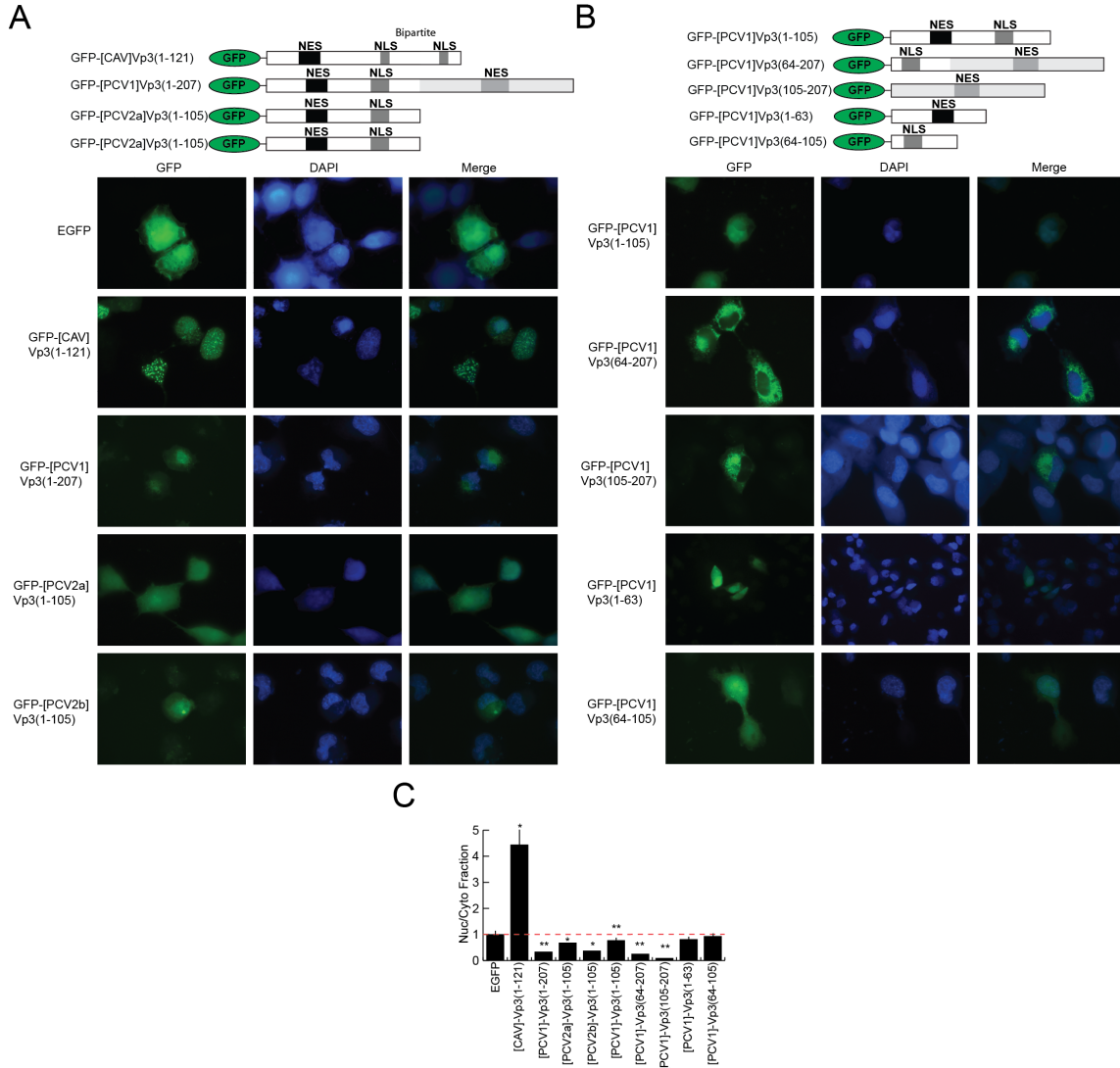


**Figure 5: Fluorescence microscopy of N-Terminal tagged GFP fusion proteins demonstrates a non-nuclear localization.**

(A) Epifluorescence microscopy of GFP-VP3 fusion proteins demonstrates VP3 of PCV is dominantly non-nuclear protein. (B) Truncation mutants of PCV1 VP3 demonstrate a functioning NES in the tail of PCV1. The forward NES predicted and the putative NLS appear to be non-functional. (C) The Nuclear/cytoplasmic fraction for each panel was calculated by green pixel intensity in both regions and the results verified the visual interpretation (\* $P=0.05$ , \*\* $P=0.005$ ).

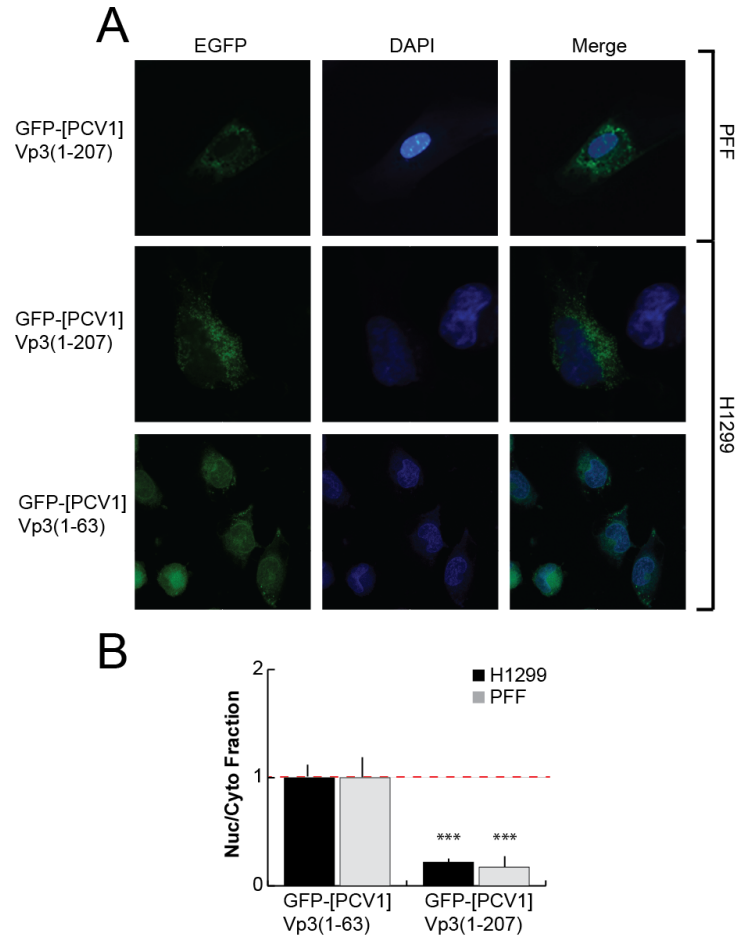


**Figure 6: Subcellular localization of PCV1 VP3 does not differ between primary and transformed cells.**

(A) GFP tagged wild type PCV1 VP3 expressed in PFF and H1299 cells demonstrated non-nuclear localization in both cell types. (B) The nucleo/cytoplasmic fraction was calculated as before confirming the visual results (\*\*\*) $P < 0.0005$ .

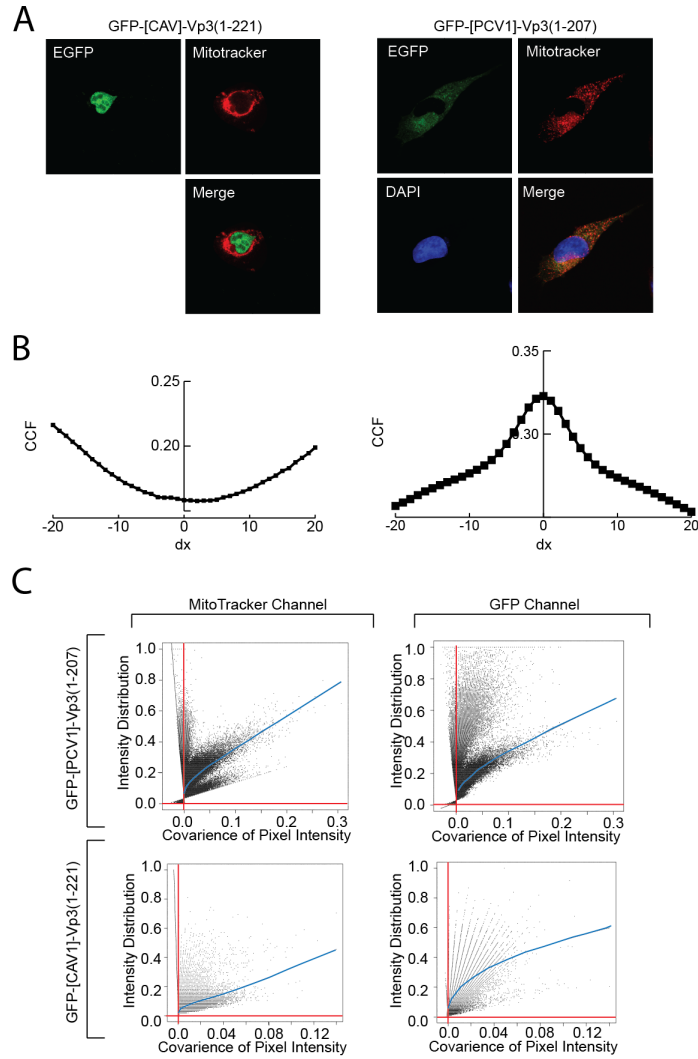


**Figure 7: Mitotracker results indicated there was a potential for mitochondrial localization.**

(A) Confocal microscopy of GFP tagged CAV Apoptin and PCV1 VP3. Invitrogen Mito Tracker® stain was used to determine mitochondrial localization. (B) Van Steensel's Cross Correlation Function (CCF) was used to determine potential co-localization of PCV1 VP3 in the mitochondria. The peak near dx=0 for PCV1 VP3 suggests potential co-localization, but the peak value is not large enough to be definitive. (C) Li's Intensity Correlation Analysis was used to supplement data obtained from Van Steensel's CCF. The results suggest a potential of co-localization but further experimentation is required.

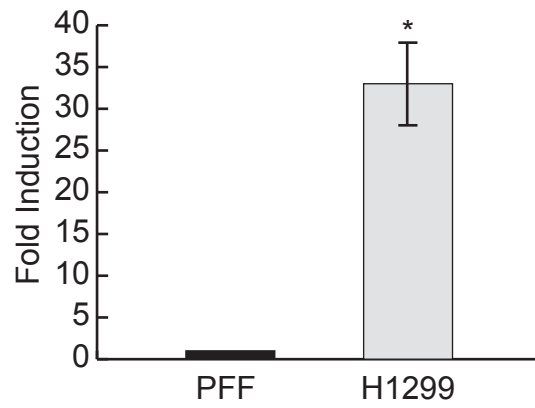


**Figure 8: Apoptosis induction is selective to transformed cells.**

Apoptosis assays showed a 33-fold increase in apoptosis induction in transformed lines over primary cells.

## References

1. **Aas T., A. L. Børresen, S. Geisler, B. Smith-Sørensen, H. Johnsen, J. E. Varhaug, L. A. Akslen, and P. E. Lønning.** 1996. Specific P53 mutations are associated with de novo resistance to doxorubicin in breast cancer patients. *Nature Medicine* **2**:811–814.
2. **Adam S. A., and L. Geracet.** 1991. Cytosolic proteins that specifically bind nuclear location signals are receptors for nuclear import. *Cell* **66**:837–847.
3. **Aghi M., T. C. Chou, K. Suling, X. O. Breakefield, and E. A. Chiocca.** 1999. Multimodal cancer treatment mediated by a replicating oncolytic virus that delivers the oxazaphosphorine/rat cytochrome P450 2B1 and ganciclovir/herpes simplex virus thymidine kinase gene therapies. *Cancer Research* **59**:3861.
4. **ALVISI G., I. POON, and D. JANS.** 2006. Tumor-specific nuclear targeting: Promises for anti-cancer therapy? *Drug Resistance Updates* **9**:40–50.
5. **Ames B. N.** 2001. DNA damage from micronutrient deficiencies is likely to be a major cause of cancer. *Mutation Research/Fundamental and Molecular Mechanisms of Mutagenesis* **475**:7–20.
6. **Baek K.-H., A. Zaslavsky, R. C. Lynch, C. Britt, Y. Okada, R. J. Siarey, M. W. Lensch, I.-H. Park, S. S. Yoon, T. Minami, J. R. Korenberg, J. Folkman, G. Q. Daley, W. C. Aird, Z. Galdzicki, and S. Ryeom.** 2009. Down's syndrome suppression of tumour growth and the role of the calcineurin inhibitor DSCR1. *Nature* **459**:1126–1130.
7. **Bold R. J., P. M. Termuhlen, and D. J. McConkey.** 1997. Apoptosis, cancer and cancer therapy. *Surgical oncology* **6**:133–142.
8. **Bolte S., and F. P. Cordelières.** 2006. A guided tour into subcellular colocalization analysis in light microscopy. *J Microsc* **224**:213–232.
9. **Buja L. M., M. L. Eigenbrodt, and E. H. Eigenbrodt.** 1993. Apoptosis and necrosis. Basic types and mechanisms of cell death. *Arch. Pathol. Lab. Med.* **117**:1208–1214.
10. **Chaiyakul M., K. Hsu, R. Dardari, F. Marshall, and M. Czub.** 2010. Cytotoxicity of ORF3 Proteins from a Nonpathogenic and a Pathogenic Porcine Circovirus. *J. Virol.* **84**:11440–11447.
11. **Chipuk J. E., and D. R. Green.** 2008. How do BCL-2 proteins induce mitochondrial outer membrane permeabilization? *Trends in Cell Biology* **18**:157–164.
12. **Cordeli F.** 2008. JACoP v2. 0: improving the user experience with co-localization studies. *ImageJ User and Developer Conference.*
13. **Cornelis J. J., N. Salomé, C. Dinsart, and J. Rommelaere.** 2004. Vectors based on autonomous parvoviruses: novel tools to treat cancer? *J Gene Med* **6 Suppl 1**:S193–202.
14. **Crowther R., J. Berriman, and W. Curran.** 2003. Comparison of the Structures of Three Circoviruses: Chicken Anemia Virus, Porcine Circovirus Type 2, and Beak and Feather Disease Virus. *Journal of ...*
15. **Danen-Van Oorschot A., D. Fischer, J. Grimbergen, B. Klein, S. Zhuang, J. Falkenburg, C. Backendorf, P. Quax, A. van der Eb, and M. Noteborn.** 1997. Apoptin induces apoptosis in human transformed and malignant cells but not in normal cells. *PNAS* **94**:5.
16. **Eheman C., S. J. Henley, R. Ballard-Barbash, E. J. Jacobs, M. J. Schymura, A.-M. Noone, L. Pan, R. N. Anderson, J. E. Fulton, B. A. Kohler, A. Jemal, E. Ward, M. Plescia, L. A. G. Ries, and B. K. Edwards.** 2012. Annual Report to the Nation on the status of cancer, 1975-2008, featuring cancers associated with excess weight and lack of sufficient physical activity. *Cancer* **118**:2338–2366.
17. **Finsterbusch T., T. Steinfeldt, K. Doberstein, C. Rödner, and A. Mankertz.** 2009. Interaction of the replication proteins and the capsid protein of porcine circovirus type 1 and 2 with host proteins. *Virology* **386**:122–131.
18. **Fisher D. E.** 1994. Apoptosis in cancer therapy: crossing the threshold. *Cell* **78**:539–542.
19. **Fulda S., and K.-M. Debatin.** 2006. Extrinsic versus intrinsic apoptosis pathways in anticancer chemotherapy. *Oncogene* **25**:4798–4811.
20. **Gatenby R. A., and P. Maini.** 2003. Cancer summed up. *Nature* **421**.
21. **Görlich D., and U. Kutay.** 1999. Transport between the cell nucleus and the cytoplasm. *Annual*

- review of cell and developmental biology **15**:607–660.
22. **Heilman D. W., Heilman D. W., J. G. Teodoro, J. G. Teodoro, M. R. Green, and M. R. Green.** 2006. Apoptin Nucleocytoplasmic Shuttling Is Required for Cell Type-Specific Localization, Apoptosis, and Recruitment of the Anaphase-Promoting Complex/Cyclosome to PML Bodies. *J. Virol.* **80**:7535–7545.
  23. **Heilman D., M. Green, and J. Teodoro.** 2005. The anaphase promoting complex: a critical target for viral proteins and anti-cancer drugs. *Cell cycle (Georgetown, Tex)* **4**:4.
  24. **Horton P., K. J. Park, T. Obayashi, N. Fujita, H. Harada, C. J. Adams-Collier, and K. Nakai.** 2007. WoLF PSORT: protein localization predictor. *Nucleic Acids Res.* **35**:W585–W587.
  25. **Invitrogen.** 2008. MitoTracker® Mitochondrion-Selective Probes.
  26. **Karra H., R. Pitkänen, M. Nykänen, K. Talvinen, T. Kuopio, M. Söderström, and P. Kronqvist.** 2012. Securin predicts aneuploidy and survival in breast cancer. *Histopathology.*
  27. **Kokolis J., and L. Spada.** 2010. Assessing the Functionality of Localization Sequences Isolated from PCV1 VP3. Worcester Polytechnic Institute, Worcester.
  28. **Kucharski T. J., I. Gamache, O. Gjoerup, and J. G. Teodoro.** 2011. DNA damage response signaling triggers nuclear localization of the chicken anemia virus protein apoptin. *J. Virol.* **85**:12638–12649.
  29. **la Cour T., R. Gupta, K. Rapacki, K. Skriver, F. M. Poulsen, and S. Brunak.** 2003. NESbase version 1.0: a database of nuclear export signals. *Nucleic Acids Res.* **31**:393–396.
  30. **la Cour T., L. Kiemer, A. Mølgaard, R. Gupta, K. Skriver, and S. Brunak.** 2004. Analysis and prediction of leucine-rich nuclear export signals. *Protein Eng. Des. Sel.* **17**:527–536.
  31. **Larkin M. A., G. Blackshields, N. P. Brown, R. Chenna, P. A. McGettigan, H. McWilliam, F. Valentin, I. M. Wallace, A. Wilm, R. Lopez, J. D. Thompson, T. J. Gibson, and D. G. Higgins.** 2007. Clustal W and Clustal X version 2.0. *Bioinformatics* **23**:2947–2948.
  32. **Li P., D. Nijhawan, I. Budihardjo, S. M. Srinivasula, M. Ahmad, E. S. Alnemri, and X. Wang.** 1997. Cytochrome c and dATP-dependent formation of Apaf-1/caspase-9 complex initiates an apoptotic protease cascade. *Cell* **91**:479–489.
  33. **Liu J., I. Chen, and J. Kwang.** 2005. Characterization of a previously unidentified viral protein in porcine circovirus type 2-infected cells and its role in virus-induced apoptosis. *J. Virol.* **79**:8262–8274.
  34. **Liu W., X. Dong, M. Mai, R. S. Seelan, K. Taniguchi, K. K. Krishnadath, K. C. Halling, J. M. Cunningham, C. Qian, E. Christensen, P. C. Roche, D. I. Smith, and S. N. Thibodeau.** 2000. Mutations in AXIN2 cause colorectal cancer with defective mismatch repair by activating  $\beta$ -catenin/TCF signalling. *Nat Genet* **26**:146–147.
  35. **Lorenzo E., C. Ruiz-Ruiz, A. J. Quesada, G. Hernández, A. Rodríguez, A. López-Rivas, and J. M. Redondo.** 2002. Doxorubicin induces apoptosis and CD95 gene expression in human primary endothelial cells through a p53-dependent mechanism. *J. Biol Chem.* **277**:10883.
  36. **Los M., S. Panigrahi, I. Rashedi, S. Mandal, J. Stetefeld, F. Essmann, and K. Schulze-Osthoff.** 2009. Apoptin, a tumor-selective killer. *BBA - Molecular Cell Research* **1793**:1335–1342.
  37. **Lowe S. W., S. Bodis, A. McClatchey, L. Remington, H. E. Ruley, D. E. Fisher, D. E. Housman, and T. Jacks.** 1994. p53 status and the efficacy of cancer therapy in vivo. *Science* **266**:807–810.
  38. **Mooi W., and D. Peeper.** 2006. Oncogene-induced cell senescence—halting on the road to cancer. *N Engl J Med* **355**:1037–1046.
  39. **Nagata S.** 2000. Apoptotic DNA fragmentation. *Exp. Cell Res.* **256**:12–18.
  40. **Nagata S.** 1999. Fas ligand-induced apoptosis. *Annu. Rev. Genet.* **33**:29–55.
  41. **Noteborn M. H., D. Todd, C. A. Verschueren, H. W. de Gauw, W. L. Curran, S. Veldkamp, A. J. Douglas, M. S. McNulty, A. J. van der Eb, and G. Koch.** 1994. A single chicken anemia virus protein induces apoptosis. *J. Virol.* **68**:346–351.
  42. **Okabe Y.** 2005. Toll-like receptor-independent gene induction program activated by mammalian DNA escaped from apoptotic DNA degradation. *Journal of Experimental Medicine* **202**:1333–1339.
  43. **Orrenius S., B. Zhivotovsky, and P. Nicotera.** 2003. Regulation of cell death: the calcium-apoptosis link. *Nat. Rev. Mol. Cell Biol.* **4**:552–565.
  44. **Paris M., and M. Zelic.** 2011. Subcellular Localization Analysis of Truncation Mutants of Porcine Circovirus 1 VP3. Worcester Polytechnic Institute.

45. **Phenix K. V., J. H. Weston, I. Ypelaar, A. Lavazza, J. A. Smyth, D. Todd, G. E. Wilcox, and S. R. Raidal.** 2001. Nucleotide sequence analysis of a novel circovirus of canaries and its relationship to other members of the genus *Circovirus* of the family *Circoviridae*. *J Gen Virol* **82**:2805–2809.
46. **Pipas J. M.** 2009. SV40: Cell transformation and tumorigenesis. *Virology* **384**:294–303.
47. **Pringle C.** 1999. Virus taxonomy at the XIth International Congress of Virology, Sydney, Australia, 1999. *Arch Virol* **144**:2065–2070.
48. **Promega Corporation.** 2009. Apo-ONE(R) Homogeneous Caspase-3/7 Assay Technical Bulletin, TB295 1–18.
49. **Promega Corporation.** 2010. PureYield(TM) Plasmid Midiprep System Technical Manual, TM253.
50. **Qiagen.** 2002. Transfection Reagent Handbook. Qiagen.
51. **Sachs L., and J. Lotem.** 1993. Control of programmed cell death in normal and leukemic cells: new implications for therapy. *Blood* **82**:15–21.
52. **Sherr C. J.** 2004. Principles of tumor suppression. *Cell* **116**:235–246.
53. **Shuai J., W. Wei, L. Jiang, X. L. Li, N. Chen, and W. Fang.** 2008. Mapping of the nuclear localization signals in open reading frame 2 protein from porcine circovirus type 1. *Acta Biochimica et Biophysica Sinica* **40**:71–77.
54. **Sporn M. B., and G. J. Todaro.** 1980. Autocrine secretion and malignant transformation of cells. *N Engl J Med* **303**:878–880.
55. **Teodoro J. G., D. W. Heilman, A. E. Parker, and M. R. Green.** 2004. The viral protein Apoptin associates with the anaphase-promoting complex to induce G2/M arrest and apoptosis in the absence of p53. *Genes & Development* **18**:1952–1957.
56. **Tischer I., L. Bode, D. Peters, S. Pociuli, and B. Germann.** 1995. Distribution of antibodies to porcine circovirus in swine populations of different breeding farms. *Arch Virol* **140**:737–743.
57. **Tischer I., D. Peters, R. Rasch, and S. Pociuli.** 1987. Replication of porcine circovirus: induction by glucosamine and cell cycle dependence. *Arch Virol* **96**:39–57.
58. **Tischer I., and R. Rasch.** 1974. Characterization of papovavirus-a... [Zentralbl Bakteriolog Orig A. 1974] - PubMed - NCBI. *Zentralblatt für Bakteriologie*.
59. **Warters R. L.** 1992. Radiation-induced apoptosis in a murine T-cell hybridoma. *Cancer Research* **52**:883.
60. **Wu Z., Y. Lin, H. Xu, H. Dai, M. Zhou, S. Tsao, L. Zheng, and B. Shen.** 2011. High risk of benzo [α] pyrene-induced lung cancer in E160D FEN1 mutant mice. *Mutation Research/Fundamental and Molecular Mechanisms of Mutagenesis*.
61. **Xu G., and Y. Shi.** 2007. Apoptosis signaling pathways and lymphocyte homeostasis. *Cell Res* **17**:759–771.
62. **Yee K. S.** 2005. Complicating the complexity of p53. *Carcinogenesis* **26**:1317–1322.
63. **Zink D., A. H. Fische, and J. A. Nickerson.** 2004. Nuclear structure in cancer cells. *Nat Rev Cancer* **4**:677–687.
64. **2005. Virus Taxonomy VIIIth Report of the International Committee on Taxonomy of Viruses VIII.** Academic Press, New York.